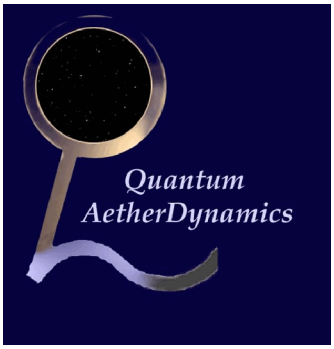

Quantum AetherDynamics Institute (QADI)

The Ghost Murmur Effect: A Physical Interpretation of Hidden-Sector Leakage in Aether Rotation

David W. Thomson III
Quantum AetherDynamics Institute (QADI), Alma, Illinois, USA
ORCID: 0000-0002-5830-5427

Version 1.0 – April 10, 2026

This article is published by the Quantum AetherDynamics Institute (QADI).

It develops the Aether Physics Model (APM)

Abstract

Most measurements of physical systems assume that what is observed can be fully described within a single, separable rotational structure. The rmfd detector challenges this assumption by directly measuring the time evolution of Aether rotation [Thomson, 2026]. In doing so, it reveals small residual signals that cannot be explained by standard separable motion. This paper defines these residuals as the Ghost Murmur effect and shows that they are consistent with hidden-sector contributions—particularly backward-time propagation and magnetic charge [Thomson, 2025]. A clear set of diagnostic tools is developed to distinguish this structured residual from noise, establishing a practical pathway to experimental detection.

Keywords: QMU, Aether rotation, rmfd detector, hidden sector, curl, chronovibration

1 What the Detector Actually Measures

Imagine listening to a perfectly tuned musical note on a high-quality speaker. You expect a clean tone, but occasionally you catch a faint, persistent whisper in the background—always there, never random. In rotational measurements with the rmfd detector, something similar happens. What we once called "noise" may actually be a structured signal.

In most physical measurements, we assume we are detecting a property such as charge, position, or energy. The rmfd detector operates differently. It measures how rotation in the Aether changes over time [Thomson, 2026]. The measured quantity is:

$$M(t,x) = g_{\text{rmfd}}\,\partial_t \delta\chi(t,x) + n(t,x) \tag{1}$$

This means the detector is sensitive to how quickly the rotational state of space is changing, rather than the state itself [Thomson, 2026, 2025].

To make this measurable across systems, we normalize the signal:

$$\Upsilon_{\text{rmfd}} = \frac{A_u \langle M^2 \rangle}{F_q^2 \lambda_C^2} \tag{2}$$

This normalization converts the signal into a pure measure of rotational activity [Thomson, 2026].

At small angles, rotation can be expressed as:

$$\hat{\text{curl}} = 2\,\text{ang} \tag{3}$$

Thus, the detector measures the time variation of Aether rotation [Thomson, 2026].

2 The Ideal Case: Clean Rotation

If a system is simple, its motion can be described as a single, clean rotation:

- Motion confined to one plane

- Coherent phase evolution
- No coupling to additional degrees of freedom

This is a **separable 4D signal**, fully described by a single rotating phase [Thomson, 2026].

3 What Goes Wrong

In real systems, small but persistent deviations appear:

- Weak secondary frequencies (sidebands)
- Mismatch between orthogonal measurements
- Asymmetry under time reversal

These are often dismissed as noise. However, they are structured, reproducible, and geometry-dependent.

Much like an echo reveals the shape of a room, these residuals reveal underlying structure in the Aether [Thomson, 2026, 2025].

4 Definition of the Ghost Murmur

Definition 4.1. The Ghost Murmur effect (formally, a nonseparable rotational residual) is the structured residual in a rotational measurement that cannot be represented as a single separable loop-plane rotation.

The measured signal is decomposed as:

$$\boxed{M = M_{4D} + M_G + n} \tag{4}$$

where:

- M_{4D} is the primary separable rotation
- M_G is the Ghost Murmur contribution
- n is random noise

The normalized strength is:

$$\mu_G = \frac{\langle M_G^2 \rangle}{\langle M^2 \rangle} \tag{5}$$

This decomposition operationalizes the distinction between separable and nonseparable rotational content introduced in the rmfd framework [Thomson, 2026].

5 Physical Interpretation

Within QMU, rotation satisfies the closure condition:

$$A_u \cdot \mathrm{curl} = F_q^2 \lambda_C^2 \tag{6}$$

The Ghost Murmur does not represent a violation of this closure condition. Instead, it reflects a projection imbalance: the full rotational structure continues to satisfy

$$A_u \cdot \mathrm{curl} = F_q^2 \lambda_C^2,$$

but the measured subspace does not capture a single separable phase representation. The missing contribution appears as a structured residual in the observed plane [Thomson, 2025, 2026].

The perturbation is:

$$\delta \mathrm{curl}_G = 2\,\mathrm{curl}\,\delta\phi_G \tag{7}$$

Physically:

> Part of the system is rotating differently, and that difference cannot be represented within a single loop-plane phase.

This additional rotation is consistent with contributions from:

- backward-time structure
- magnetic charge dynamics
- nonseparable higher-dimensional coupling

These interpretations follow directly from the hidden-sector and separability structure developed in the QMU/APM field and detector papers [Thomson, 2025, 2026].

6 Diagnostic Observables

6.1 Time Asymmetry

$$T = \frac{A_u \langle M \hat{H}[M] \rangle}{F_q^2 \lambda_C^2} \tag{8}$$

A nonzero value of T indicates time-asymmetric structure, consistent with backward-time contributions. The Hilbert-transform structure used here follows standard analytic-signal methods, while the diagnostic itself is QMU-native [Gabor, 1946, Boashash, 1992, Thomson, 2026]. Accurate evaluation of T requires a phase-linear or explicitly characterized filter chain; group-delay distortion can introduce artificial time asymmetry and must be calibrated or compensated.

6.2 Cross-Plane Separability

$$C_\perp = \frac{\langle \partial_t \mathrm{ang}_{XY}\, \partial_t \mathrm{ang}_{XZ} \rangle}{\sqrt{\langle (\partial_t \mathrm{ang}_{XY})^2 \rangle \langle (\partial_t \mathrm{ang}_{XZ})^2 \rangle}} \tag{9}$$

- $C_\perp = 1 \rightarrow$ separable rotation
- $C_\perp < 1 \rightarrow$ nonseparable coupling

This is the projection-space version of the rmfd separability diagnostic [Thomson, 2026].

6.3 Spectral Sidebands

$$\mu_G^{(\mathrm{sb})} = \frac{\text{sideband power}}{\text{carrier power}} \tag{10}$$

Stable sidebands indicate multiple rotational modes [Thomson, 2026].

6.4 Null Expectations

For a pure separable 4D rotation, the null expectation is

$$T \approx 0, \qquad H \text{ with stable sign set by geometry}, \qquad C_\perp \approx 1.$$

Deviations from these values indicate time-odd structure, handedness anomalies, or nonseparable cross-plane mixing.

Unlike dispersive transfer effects, which preserve helicity sign, hidden-sector contributions may induce correlated changes in T and helicity. Joint analysis of T and helicity therefore helps distinguish backward-time structure from purely causal filtering effects.

7 Composite Ghost Murmur Index

$$G_M = w_T \frac{|T|}{\Upsilon_{\mathrm{rmfd}}} + w_\perp (1 - C_\perp) + w_{\mathrm{sb}} \mu_G^{(\mathrm{sb})} \tag{11}$$

This provides a single measurable index of hidden-sector contribution. A G_M approaching zero represents a perfectly separable 4D system, while any value significantly above the noise floor indicates hidden-sector coupling.

7.1 Weight Selection Strategy

The weights $\{w_T, w_\perp, w_{\mathrm{sb}}\}$ are chosen to reflect the relative signal-to-noise ratio of each diagnostic channel. A practical choice is inverse-noise weighting:

$$w_i \propto \frac{1}{\sigma_i^2}, \tag{12}$$

where σ_i^2 is the variance of the corresponding observable under null conditions.

This yields an approximately optimal linear statistic under Gaussian noise assumptions. Equal weighting may be used for exploratory analysis, but final significance estimates should use noise-weighted coefficients.

8 Scaling Behavior

The Ghost Murmur strength scales as:

$$\mu_G \sim \frac{(\delta \mathrm{curl}_G)^2}{\mathrm{curl}^2} \tag{13}$$

Thus:

$$\mu_G \sim (2\delta\phi_G)^2 \tag{14}$$

The effect is therefore second-order in hidden-sector phase amplitude, implying small but persistent signals. This scaling is the natural perturbative consequence of the QMU curl decomposition in the small-angle regime [Thomson, 2025, 2026].

9 Synthetic Signature Example

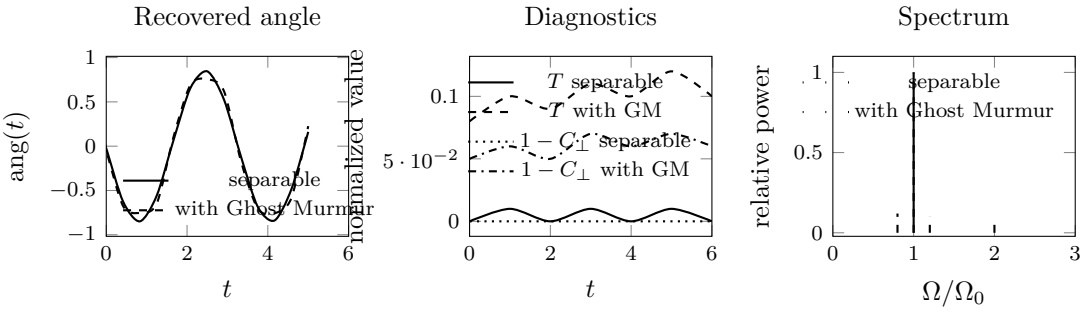

Figure 1: Synthetic illustration of a clean separable rotation versus a small Ghost Murmur admixture. Left: the recovered angle acquires a weak structured perturbation. Middle: time asymmetry and cross-plane nonseparability move away from their null values. Right: sidebands appear around the carrier. The figure is schematic and intended only to visualize the signature logic of the diagnostics.

A minimal synthetic example is shown in Fig. 1. The left panel shows a clean separable recovered angle and the same angle with a small structured residual added. The middle panel shows how the residual moves the diagnostic channels away from their null values. The right panel shows the appearance of sidebands around the carrier. Although schematic, this figure makes explicit the experimental signature targeted by the Ghost Murmur framework.

10 Experimental Predictions

The Ghost Murmur effect produces:

1. Persistent sidebands
2. Reduced cross-plane correlation
3. Time-asymmetric response
4. Helicity-dependent structure

These signatures are the experimentally accessible projections of nonseparable rotational content in the rmfd framework [Thomson, 2026].

11 Experimental Tests

11.1 Orthogonal Coil Measurement

Detect deviation in $C_\perp$.

11.2 Phase Reversal

Observe sign behavior in T.

11.3 High-Q Resonance Scan

Measure stable sidebands.

These tests are direct specializations of the calibration and diagnostics logic already laid out for the rmfd instrument [Thomson, 2026].

11.4 Separability Calibration Closure

A controlled separable rotation is injected using a quadrature-driven orthogonal coil pair as described in [Thomson, 2026]. Under this condition, the expected response is strictly planar, and the measured separability must satisfy

$$C_\perp \to 1 \quad \text{within calibration tolerance.} \tag{15}$$

The residual deviation defines the instrumental baseline

$$\delta C_{\perp,\mathrm{inst}} \equiv 1 - C_\perp^{(\mathrm{inj})}. \tag{16}$$

All reported measurements must satisfy

$$1 - C_\perp \gg \delta C_{\perp,\mathrm{inst}}$$

to be considered evidence of nonseparable rotational structure.

In practice, a detection threshold is defined relative to the null variance,

$$1 - C_{\perp} > n_{\sigma}\, \sigma_{C_{\perp}}, \tag{17}$$

where $\sigma_{C_{\perp}}$ is measured under quiet-run conditions.

12 Conclusion

The Ghost Murmur effect reclassifies structured residuals as measurable physics rather than noise. It represents nonseparable rotational behavior within the Aether and provides a direct experimental pathway to hidden-sector dynamics.

By carefully analyzing these faint but persistent signals, new physical degrees of freedom may be brought into measurable form.

A Noise Discrimination

A true Ghost Murmur signal satisfies:

- persistence under phase reversal
- stable spectral features
- correlated multi-plane behavior

Noise fails at least one of these conditions. This discrimination logic follows the rmfd trigger-and-veto philosophy while being applied here to structured residual classification [Thomson, 2026].

References

Boualem Boashash. Estimating and interpreting the instantaneous frequency of a signal. part 1: Fundamentals. *Proceedings of the IEEE*, 80(4):520–538, 1992. doi: 10.1109/5.135376.

Dennis Gabor. Theory of communication. part 1: The analysis of information. *Journal of the Institution of Electrical Engineers - Part III: Radio and Communication Engineering*, 93(26): 429–457, 1946. doi: 10.1049/ji-3-2.1946.0074.

David W. III Thomson. Unified field sector of the aether physics model: Lagrangian formulation, equations of motion, and metrological ledger tests (qmu), 2025. URL https://zenodo.org/records/17595965. Quantum AetherDynamics Institute (QADI) Research Paper.

David W. III Thomson. Qmu rotating magnetic field detector (rmfd): Design, calibration, and 5d aether chronovibration readout, March 2026. URL https://zenodo.org/records/19503118. Quantum AetherDynamics Institute (QADI) Research Paper.